

nanomedicine

Nanotechnology, Biology, and Medicine



Special Topic: Two-Dimensional Biomaterials in Regenerative Guest Editor: Manus Biggs

W. Zhu, T. Ye, S.-J. Lee, H. Cui, S. Miao, X. Zhou, D. Shuai, L.G. Zhang Nanomedicine: Nanotechnology, Biology, and Medicine, Volume 14, Number 7, Pages 2483–2492.





BASIC SCIENCE

Nanomedicine: Nanotechnology, Biology, and Medicine 14 (2018) 2485 – 2494



nanomedjournal.com

Feature Article

Special Topic: Two-Dimensional Biomaterials in Regenerative Medicine

Enhanced neural stem cell functions in conductive annealed carbon nanofibrous scaffolds with electrical stimulation

Wei Zhu, MS^{a,1}, Tao Ye, MS^{b,1}, Se-Jun Lee, BS^a, Haitao Cui, PhD^a, Shida Miao, PhD^a, Xuan Zhou, PhD^a, Danmeng Shuai, PhD^b, Lijie Grace Zhang, PhD^{a,c,d,*}

^aDepartment of Mechanical and Aerospace Engineering, The George Washington University, Washington, DC, USA

^bDepartment of Civil and Environmental Engineering, The George Washington University, Washington, DC, United States

^cDepartment of Biomedical Engineering, The George Washington University, Washington, DC, USA

^dDepartment of Medicine, The George Washington University, Washington, DC, USA

Received 14 October 2016; accepted 6 March 2017

Abstract

Carbon-based nanomaterials have shown great promise in regenerative medicine because of their unique electrical, mechanical, and biological properties; however, it is still difficult to engineer 2D pure carbon nanomaterials into a 3D scaffold while maintaining its structural integrity. In the present study, we developed novel carbon nanofibrous scaffolds by annealing electrospun mats at elevated temperature. The resultant scaffold showed a cohesive structure and excellent mechanical flexibility. The graphitic structure generated by annealing renders superior electrical conductivity to the carbon nanofibrous scaffold. By integrating the conductive scaffold with biphasic electrical stimulation, neural stem cell proliferation was promoted associating with upregulated neuronal gene expression level and increased microtubule-associated protein 2 immunofluorescence, demonstrating an improved neuronal differentiation and maturation. The findings suggest that the integration of the conducting carbon nanofibrous scaffold and electrical stimulation may pave a new avenue for neural tissue regeneration. © 2017 Elsevier Inc. All rights reserved.

Key words: Carbon nanofiber; Conductive nanomaterial; Electrical stimulation; Neural stem cell; Neural differentiation

Stem cell-based transplantation therapy has opened up new possibilities for repairing injured tissues or organs. As a multipotent cell population, neural stem cells (NSCs) are exhibiting promise for various neurodegenerative diseases and injuries. The therapeutic efficacy of NSCs is exclusive by a cell-replacement mechanism. NSC line is capable of self-renewing and differentiating into neurons and other glial cells (astrocytes and oligodendrocytes) that can integrate with host tissues and repair nerve damages by improving neurogenesis and axonal growth. The undifferentiated NSCs might also repair nerves by intrinsic neuroprotective ability in which NSCs release a series of bioactive molecules, *e.g.*, neurotrophic growth factors, immunomodulatory substances, for maintaining neural tissue homeostasis. Despite

great progression is achieved, there remains important issues that need to be solved regarding the NSC-based therapy. Direct transplantation of NSCs fails to offer the physiological stimulations that can promote proliferation and differentiation, and induce functional integration of NSC-derived neurons into healthy neural networks. ^{2,4} In order to support proper cell functions, NSCs are generally introduced to a target region by mixing with or being seeded on a functional scaffold. The functional scaffold provides mechanical support and physiochemical cues for guiding neural cell growth and differentiation as well as forming complex neural tissue patterns. ^{5,6}

Due to the intrinsic electroactivity of nerve cells, conductive scaffolds are of particular interest in neuroscience by offering means

http://dx.doi.org/10.1016/j.nano.2017.03.018

1549-9634/© 2017 Elsevier Inc. All rights reserved.

Conflict of Interest and Disclosure: N/A.

All sources of support for research: This work was supported by the March of Dimes Foundation's Gene Discovery and Translational Research Grant, and NSF MME grant #1642186.

^{*}Corresponding author at: 3590 Science and Engineering Hall, Washington, DC.

E-mail address: lgzhang@gwu.edu (L.G. Zhang).

These two authors contribute equally to this work.

to apply electrical stimulation. Carbon-based nanomaterials, including carbon nanotubes (CNTs), carbon nanofibers (CNFs), and graphene, hold potential for neural applications due to their unique electrical, mechanical, and biological properties. ^{7,8} In addition, neural tissue extracellular matrix (ECM) consists of various nanostructured components which directly interact with neural cells as well as stimulate cell growth and differentiation. In this regard, the nanoscale features of CNTs, CNFs, and graphene may provide a biomimetic nanostructured environment, which makes them superior to other conventional biomaterials in micro-macro dimension. 9 Actually, CNTs have been demonstrated to promote neuron proliferation, modulate neuronal behavior at either structural (neurite elongation) or functional (synaptic efficacy) level, as well as increase network activity of neuronal circuits. 10-12 Usmani et al found that conductive 3D CNT meshes were able to guide neural webs formation and facilitated signal transmission when cultured segregated spinal cord on them in vitro. 13 The in vivo implantation of the CNT meshes presented low tissue reaction as well. Graphene can also enhance neuronal differentiation, guide axons extension, and support functional neural circuit growth. 14-18

In addition to the enhanced neural cell behaviors by conductive scaffolds themselves, external electrical stimulation is usually employed in an effort to restore injured neural functions. Despite exact mechanism of the interactions between electrical stimulation and neural cell/system has yet to be fully understood, it has been well-documented that electrical stimulation can increase neurite outgrowth *in vitro* and enhance functional recovery *in vivo*. ^{19,20} Furthermore, electrical stimulation delivered *via* carbon-based nanomaterials has been demonstrated to induce neuronal signaling. ²¹

In the present study, conductive carbon nanofibrous scaffolds have been fabricated by annealing polymeric precursor electrospun fiber mats. Unlike the CNTs or CNFs synthesized by other methods, such as laser ablation, and chemical vapor deposition, this annealing approach can directly generate an integrated network structure in the absence of substrate for deposition and any catalyst. It was demonstrated that the electrospun carbon nanofibers (ECNFs) fabricated by annealing electrospun polymeric nanofibers can support human endometrial stem cells to give rise to neuron-like cells, ²² showing great promise in neural regeneration. Considering the advantages of conducting ECNFs and electrical stimulation on neural tissue engineering, we postulate that the combination of them will generate a robust strategy for neural regeneration. Therefore, we investigated here the electrical properties of annealed ECNFs and bioactivity by culturing NSCs. Additionally, we applied electrical stimulation on the NSC seeded ECNF scaffold; the cell proliferation was studied associating with the detection of neural differentiation by quantitative real-time polymerase chain reaction (RT-PCR) and immunocytochemistry.

Methods

Fabrication of conductive ECNF scaffolds

The ECNF scaffolds were fabricated via a single-spinneret electrospinning and post-thermal treatment similar to our previous work. ²³ In a typical procedure, 0.5 g of terephthalic

acid (PTA) was first dissolved in 10 g of N, N-dimethylformamide (DMF) by mixing at room temperature for 10 min, and next 1 g of polyacrylonitrile (PAN) was added and further mixed at 80 °C for 3 h. The prepared solution was then electrospun using a 12 mL syringe with a 25 gauge blunt needle (NNC-PN-25GA, Nano NC) at a flow rate of 1 mL.h⁻¹ (NE-300, New Era Pump Systems Inc.). The voltage of 10 kV was applied, and the syringe needle-to-collector distance was maintained at 10 cm. A rotating drum wrapped with an aluminum foil (1000 rpm) was used to collect the fibers for 4 h. The as-spun fibers were first dried in an oven (VWR Force Air Oven) at 60 °C for 1 day, then heated in a tube furnace (OTF-1200 × -80, MTI Corporation) from room temperature to 280 °C for 2 h in air for stabilization (heating rate of 2 °C min⁻¹), followed by further heated up to 1000 °C for 1 h in N₂ for carbonization (heating rate of 5 °C min⁻¹). The annealing time and temperature were optimized based on our previous study.²³

Scaffold characterization

The morphology of fibers before and after annealing was examined by scanning electron microscope (SEM, FEI Teneo LV SEM). All samples were coated with iridium for 30 s prior to imaging. Element compositions of samples were examined by energy-dispersive X-ray spectrometer (EDS). 200 fibers from at least 10 different images were analyzed for fiber diameter with ImageJ software (National Institutes of Health, USA). The Raman spectra of the samples were characterized by a Raman spectrometer (Horiba Scientific) with a 532 nm laser excitation. For the electrochemical measurement, the cyclic voltammetry was performed using potentiostat (Digi-IVY DY 2013) with a standard three-electrode electrochemical cell. The cell assembly composed of a commercial Ag/AgCl reference electrode (Sigma-Aldrich), a counter electrode of platinum, and a working electrode with phosphate buffered saline (PBS) solution at 25 °C. The voltammogram curves were observed within the potential window from -0.8 V to 0.8 V at a scan rate of 100 mV/s, starting from zero current.

NSC culture

Mouse NSCs were obtained from ATCC (NE-4C). The cells were cultured in Eagle's Minimum Essential Medium (ATCC) supplemented with 2 mM L-Glutamine (Thermo Fisher) and 10% fetal bovine serum (FBS, Gemini) and maintained in a humidified atmosphere with 5% CO₂ at 37 °C. Cell expansion was conducted on 15 μ g/mL poly-L-lysine coated flasks. Passages 4 to 6 cells were used for all experiments. For NSC differentiation, cells were cultured in a differentiation medium composed of complete culture medium with 10^{-6} M retinoic acid (Sigma–Aldrich).

NSC viability study

To evaluate the biocompatibility of ECNFs, NSCs were cultured on ECNF scaffolds. PAN scaffolds and glass were selected as controls. Prior to cell seeding, 12 mm diameter samples were fixed on the bottom and rinsed with 70% ethanol for 20 min. After washing three times with PBS, samples were pre-wetted with complete medium overnight. NSCs were then

Table 1
The primer sequences used in RT-PCR.

Gene	Forward primer	Reverse primer	
GAPDH	GTGGCCTCTGGGATGATG	ACTCCTCAGCAACTGAGGG	
Nestin	GTGGCCTCTGGGATGATG	TTGACCTTCCTCCCCTC	
Tuj1	AGCTGTTCAAACGCATCTCG	GACACCAGGTCATTCATGTTGC	
GFAP	CCTTCCTTCCCTGGTTTTCT	TGCTCATCTTTCCTCTTCCC	
MAP2	TTCTCCACTGTGGCTGTTTG	GAGCCTGTTTGTAGACTGGAAGA	

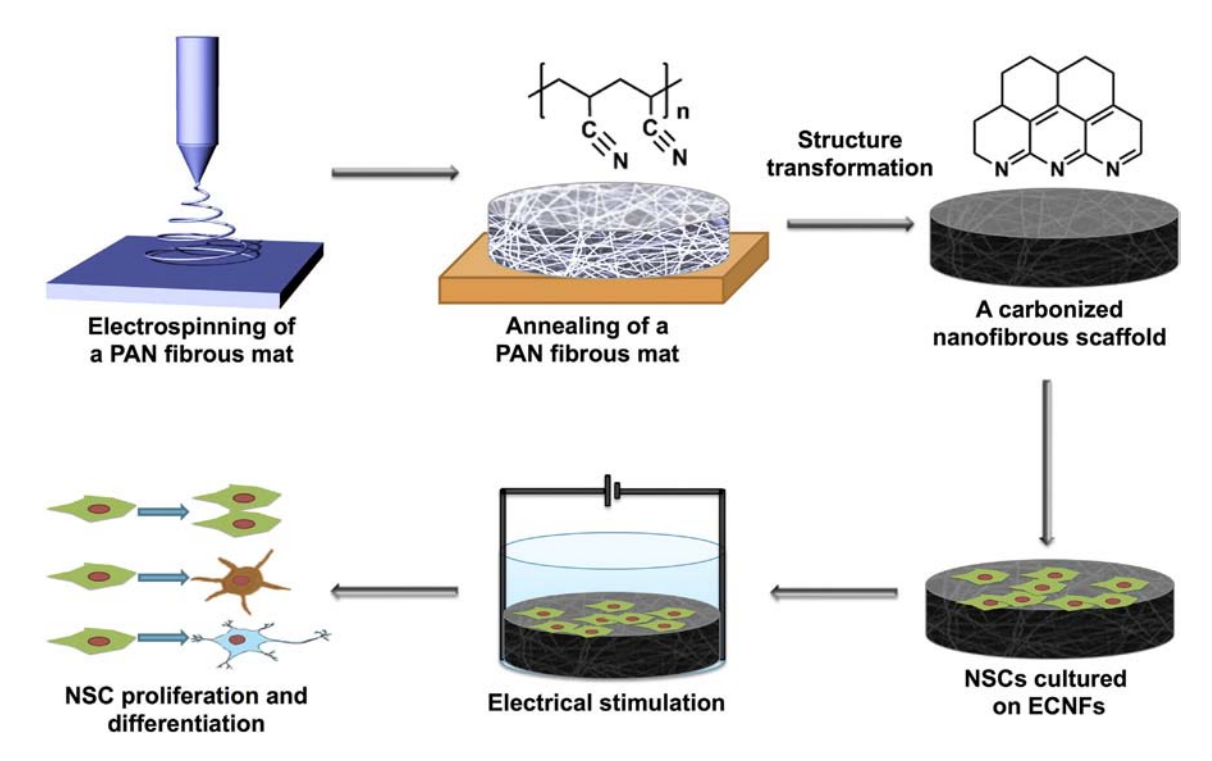


Figure 1. Schematic illustration of ECNF scaffold fabrication and electrical stimulation of NSCs on the scaffold.

seeded at a density of 10⁵ cells each sample. Cells were cultured for 2 days and then the cell growth morphology was examined by staining cells with nestin marker. Specifically, samples were fixed with 10% formalin for 15 min followed by permeabilization with 0.2% Triton X-100 (Sigma-Aldrich) for 5 min. Diluted primary antibody rabbit anti-nestin (1:500, Abcam) was gently added and incubated at 4 °C for 48 h. Secondary antibody donkey Anti-Rabbit IgG H&L (Alexa Fluor 647, Abcam) was incubated with cells for 1 h at room temperature. Cell nuclei were then stained with DAPI (4',6-Diamidino-2-Phenylindole, Sigma-Aldrich) for 5 min. The imaging was conducted using a laser scanning confocal microscope (LSCM 710, Zeiss). The actin-cytoskeleton images were used to quantify the cell shape descriptors by using ImageJ software (particle analyzer plugin). At least three samples each group were selected to perform the quantification.

In vitro electrical stimulation and NSC proliferation

The electrical stimulation device was developed in our lab which fits a standard 24-well plate. The customized electrical stimulator setup is comprised of an asymmetric biphasic programmable electrical device and a printed circuit board,

which provides robust connections of the platinum electrodes. Two platinum electrodes were positioned in each well and ensured uniform stimulation. For proliferation study, NSCs were seeded on ECNF scaffolds at a density of 10^5 cells per sample. As control, NSCs were also cultured in PAN scaffolds. After 24 h of incubation, the medium was replaced and cells were exposed to an electrical current of $100~\mu\text{A}$ and pulse rates of 100~Hz with $100~\mu\text{sec}$ duration for another 24 h. Cell number was then quantified by cell counting kit-8 (CCK-8, Dojindo) according to the manufacturer's instructions. Briefly, cells were first washed with PBS three times. Afterwards, fresh medium was added with 10% CCK-8 solution and incubated for 3 h. $100~\mu\text{L}$ medium was then transferred to a 96-well plate. Absorbance was measured at 470 nm by a spectrophotometer (Thermo Scientific Multiskan GO).

RT-PCR analysis

The gene expression of NSCs cultured on ECNF scaffold and stimulated with electrical stimulation was analyzed by RT-PCR. After 7 day incubation in a differentiation medium, the total RNA of each sample was isolated using Trizol reagent (Life Technologies), according to manufacturer's instructions. The RNA was

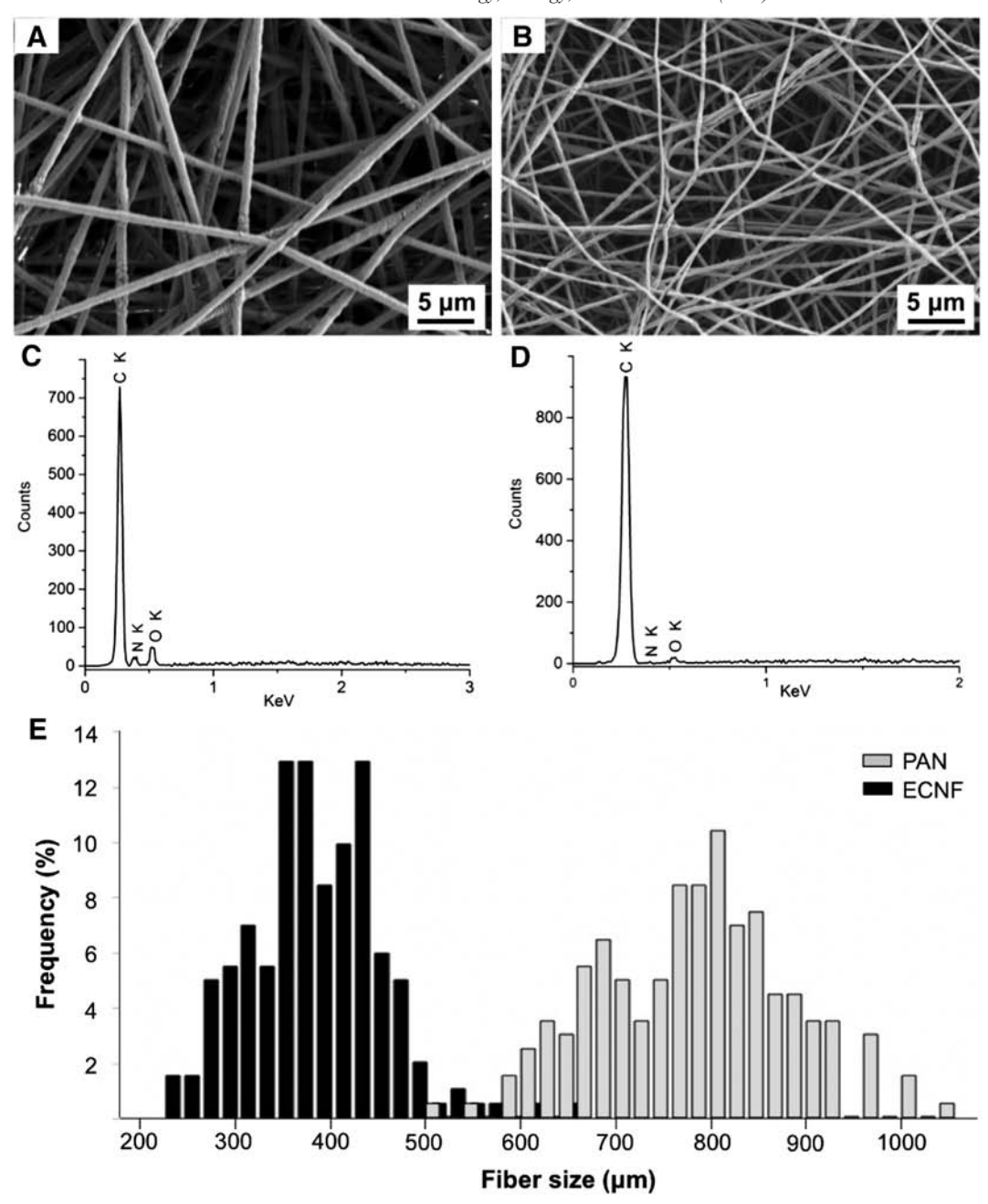


Figure 2. SEM micrographs of **(A)** as-spun PAN and **(B)** annealed ECNF scaffolds, and **(C** and **D)** EDS elemental analyses of respective scaffolds. **(E)** The fiber diameter distribution of the PAN and ECNF scaffolds.

Table 2 Elemental compositions of PAN and ECNFs.

	Sample	Carbon	Nitrogen	Oxygen
Atomic %	PAN	69.7	18.0	12.2
	ECNF	90.1	4.3	5.6
Weight %	PAN	65.1	19.6	15.2
	ECNF	87.8	4.9	7.3

then reverse-transcribed to complementary DNA (cDNA) by using a Prime-ScriptTM reagent kit (TaKaRa). The obtained cDNA was used in SYBR Green qPCR assay (TaKaRa) for gene expression

quantification. Data were normalized to the expression of the housekeeping gene glyceraldehyde-3-phosphate-dehydrogenase (GAPDH). The primers are listed in Table 1.

Immunocytochemistry analysis

NSCs were cultured on ECNF scaffolds with and without electrical stimulation for 7 days in a differentiation medium. Immunocytochemical characterization was then performed after fixing cells in 10% formalin for 15 min. NSCs grown on ECNF scaffolds were stained with specific neuronal marker. In brief, fixed

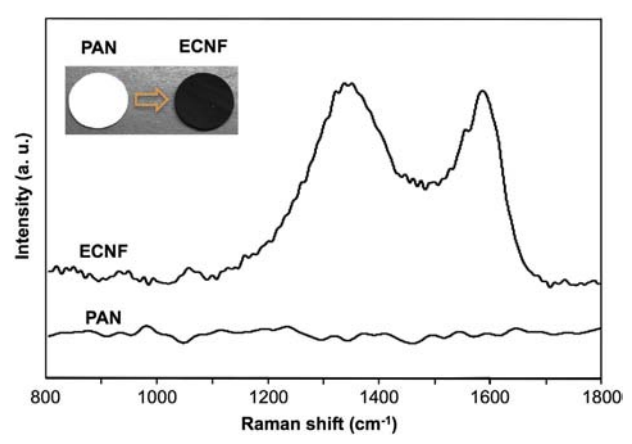


Figure 3. Raman spectra of the PAN and ECNF scaffolds. The inset shows the scaffold before and after carbonization.

cells were maintained 0.2% Triton X-100 5 min followed by blocking with 1% bovine serum albumin (BSA), 22.52 mg/mL glycine in PBST (PBS + 0.1% Tween 20) for 1 h at room temperature. The primary antibody, anti-MAP2 (microtubuleassociated protein 2) antibody (1:500, Abcam) was then incubated with cells for 48 h at 4 °C. After PBS washes, the second antibody (Alexa Fluor 647) was added and incubated with cells for another 1 h at room temperature. Nuclei were stained by DAPI. Cell imaging was performed by confocal microscopy. MAP2 relative expression and neurite length were analyzed by ImageJ software and the NeuriteTracer plugin. This plugin allows easy semi-automatic tracing of neurons through immunostaining images and to export the details of total neurite length. The relative MAP2 expression area was also calculated by counting the ratio of MAP2 positive area to the whole area of immunostaining image using ImageJ software. Three samples were selected randomly for this calculation.

Statistics

All quantitative data are expressed as mean \pm standard deviation. Statistical analysis was performed using student's t test. P < 0.05 was considered as statistical significance.

Results

Physicochemical properties of scaffolds

Figure 1 shows the schematic illustration of ECNF preparation, NSC culture, and electrical stimulation treatment. ECNFs were obtained after stabilization and carbonization of as-spun PAN fibers. Figure 2, A and B show SEM images of as-spun PAN fibers and ECNFs. The diameter of as-spun PAN fibers range from 500 to 1100 nm with an average of 780 ± 99 nm (Figure 2, C). After annealing, the fibrous mat became compact and the average diameter of fibers dramatically decreased to 384 ± 99 nm with a range from 200 to 600 nm (Figure 2, C).

The elemental composition analyses revealed that atomic and weight percentage of carbon greatly increased from 69.7% and 65.1% to 90.1% and 87.8%, respectively (Table 2). Nitrogen content

decreased from 18% to 4.3% in atomic percentage, and 19.6% to 4.9% in weight percentage. These results indicated that carbonization led to a chemical structure change of PAN to an analog of CNTs. 24,25

ECNFs produced by electrospinning PAN solution are usually brittle and rigid, and the mechanical weakness largely limits their use as an integrated network structure for engineering scaffold. ^{24,26} With the addition of PTA in the PAN solution, the flexibility and porosity of ECNFs were significantly enhanced. As shown in Supplementary movies 1 and 2, ECNFs maintain their structural integrity and cohesive structure of the as-spun PAN fibers after annealing at elevated temperature.

The Raman spectra illustrate chemical characteristics presenting on fibrous scaffolds before and after carbonization (Figure 3). In the heat treatment step, the scaffolds changed their color from white to opaque black. The D-band at 1350 cm⁻¹ associating with disordered graphite, and G-band at 1582 cm⁻¹ corresponding to ordered graphite are apparent for ECNF scaffolds, whereas no signal was detected in the PAN scaffolds before carbonization. ECNFs fabricated from annealing the as-spun PAN scaffolds are electrical conductive, as illustrated by the activated light-emitting diode (LED) (Figure 4, *A*, supporting movie 2). Figure 4, *B* shows a cyclic voltammogram curve of the ECNF scaffold. The relatively rectangular profile indicates that annealed ECNFs have excellent electronic properties. Two well-defined peaks are evident where the peak potential separation is around 0.6 V.

In vitro biocompatibility and NSC proliferation with electrical stimulation

In order to determine if the ECNF scaffold can support cell viability and growth, mouse NSCs were seeded onto ECNF scaffolds. The cell growth morphology was examined and compared with that on the PAN scaffold and glass controls. Over the course of 2 days, NSCs remained viable on ECNF and PAN scaffolds as illustrated by the expression of nestin in all groups (Figure 5, A). However, when compared to cells on glass with a confluent irregular shape, there is a distinct difference in the morphology of cells grown on the PAN scaffold, where NSCs exhibit round morphology and less nestin expression (Figure 5, B). In contrast, cells on ECNF scaffold developed into elongated morphology which is analogous to that of on glass.

Improved NSC proliferation under electrical stimulation

It was indicated that the electrical stimulation could influence cell adhesion and proliferation of stem cells. ²⁷ In this study, a 100 μA direct current was selected to stimulate cells on PAN and ECNF scaffolds. The scheme of stimulating device is shown in Figure 6, *A*. Our results revealed that the NSC proliferation on conductive ECNF scaffolds was significantly higher than that without electrical stimulation and the non-conductive PAN scaffold after 24 h stimulation (Figure 6, *B*). The cell proliferation rate on ECNF scaffolds with electrical stimulation increased 35%, 31%, and 47% when compared to cells on ECNFs without electrical stimulation, PAN with electrical stimulation, and PAN without electrical stimulation. There is no significant difference of cell proliferation when electrical stimulation was conducted on non-conductive PAN scaffolds.

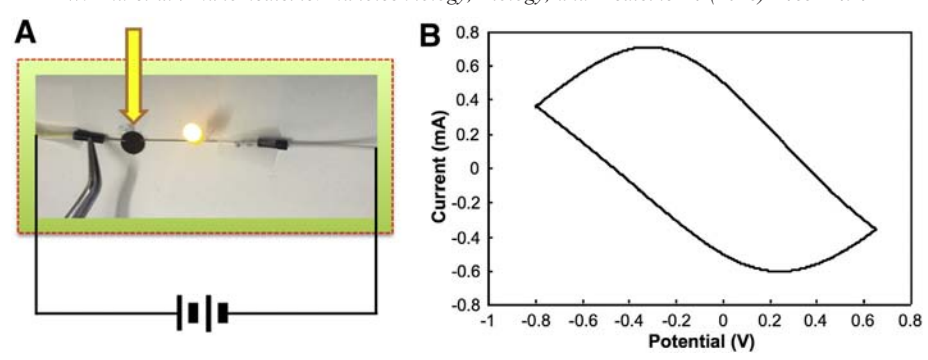


Figure 4. Electrochemical properties of the ECNF scaffold. (A) Demonstration of electrical conductivity, showing an ECNF scaffold incorporated into a circuit with an LED. Yellow arrow highlights the punched ECNF scaffold. (B) Cyclic voltammogram of the ECNF scaffold.

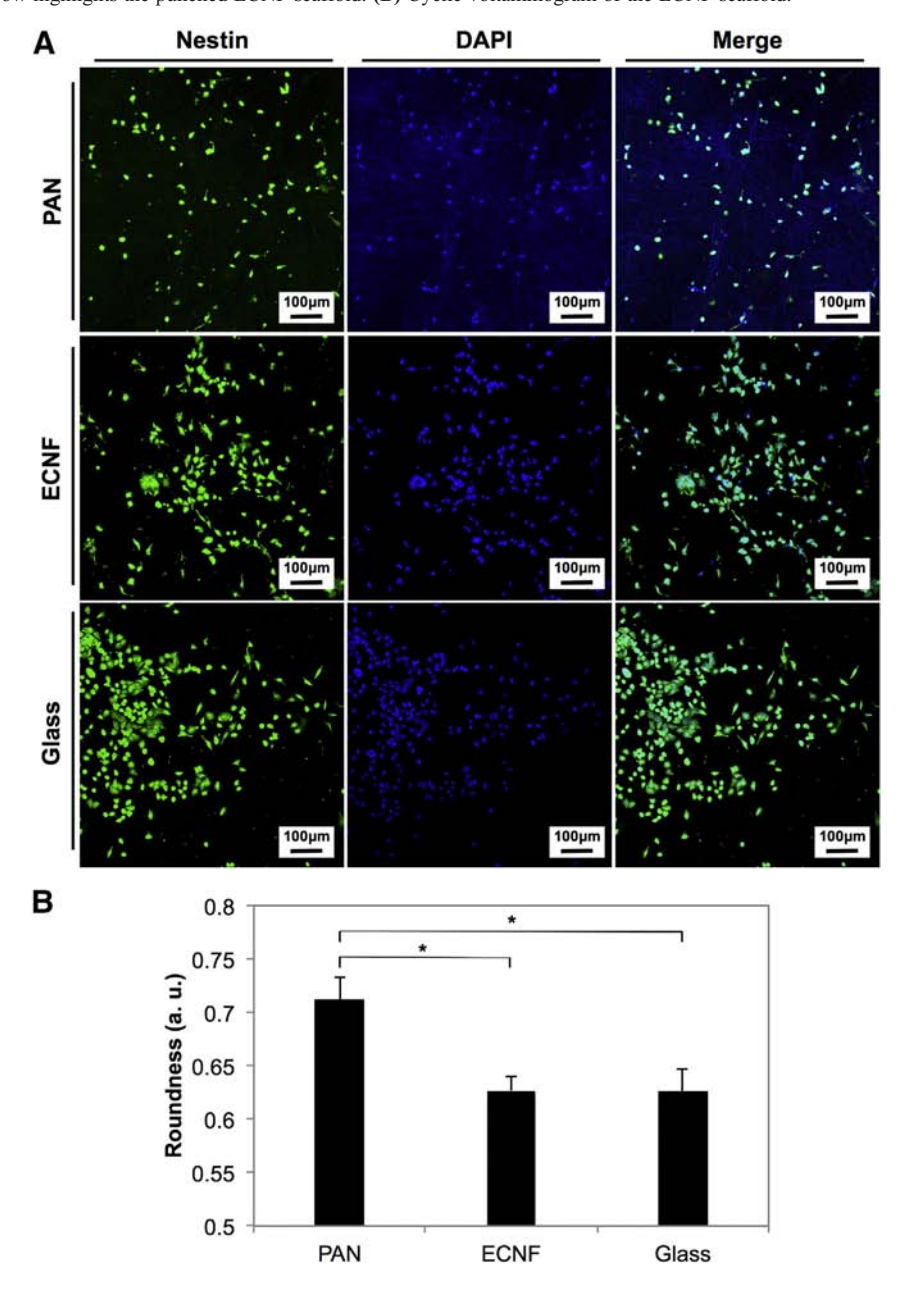


Figure 5. (A) NSC growth on various scaffolds indicating the excellent biocompatibility of ECNF scaffolds. (B) Roundness of cells on various scaffolds (calculated by ImageJ software), cells on PAN scaffold presented a distinct difference in the morphology as indicated by the higher roughness when compared to that on glass, whereas cells on ECNF scaffold developed into elongated morphology which is analogues to that of on glass. Data are reported as mean \pm standard deviation, n = 3, *P < 0.05.

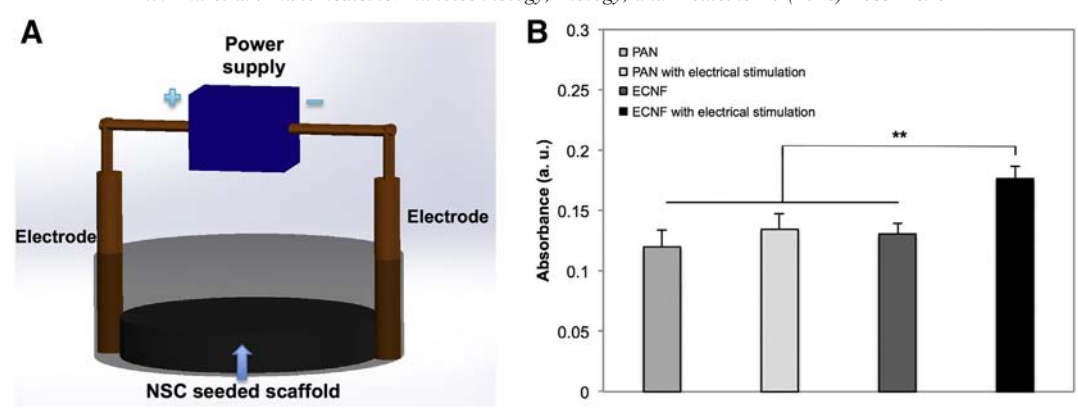


Figure 6. (A) Design of an electrical stimulation device for stimulating the electroactive ECNF scaffold, NSC seeded scaffold is placed between two electrodes which provide a biphasic current supply. (B) NSC proliferation on PAN and ECNF scaffolds with and without electrical stimulation. When electrical stimulation was performed to NSCs on various scaffolds, only the conductive ECNF group presented significantly increased cell proliferation rate. Data are reported as mean \pm standard deviation, n = 6, **P < 0.01.

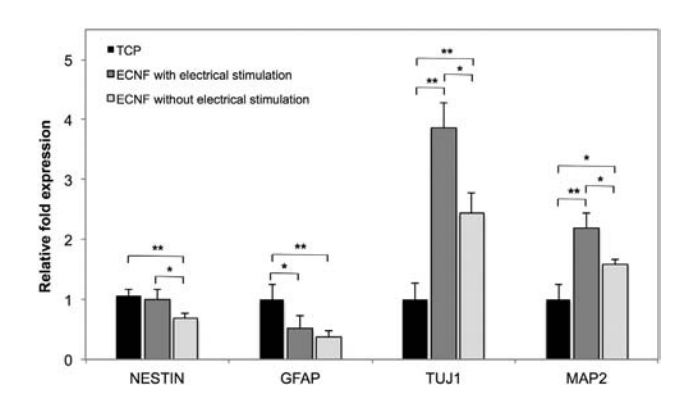


Figure 7. Gene expressions of NSCs on ECNF scaffolds with or without electrical stimulation when compared to TCPs for 7 days of culture. The data were normalized to the expression levels of cells on TCPs. Data are reported as mean \pm standard deviation, n = 4, *P < 0.05, **P < 0.01.

Enhanced neuronal differentiation and maturation under electrical stimulation

To investigate the effect of electrical stimulation through ECNF scaffolds on NSC fate during differentiation, cells were cultured in a differentiation medium and the expression patterns of glial and neurogenic genes, nestin, glial fibrillary acidic protein (GFAP), neuron-specific class III β-tubulin (Tuj1) and MAP2, were analyzed after 7 days of culture. The results indicate that the differentiation of NSCs on ECNF scaffolds was significantly different from that on tissue culture plates (TCPs) (Figure 7). The cells cultured on ECNF scaffolds, regardless of with electrical stimulation or not, showed a significant higher expression of Tuil and MAP2 when compared to those grown on TCPs. The highest expression of these two genes was observed on ECNF scaffolds in the presence of electrical stimulation. There was a 3.9-fold increase in expression of Tuj1, an early stage neuronal differentiation marker, on ECNF scaffolds with electrical stimulation in comparison with TCP controls. Tuj1 expression on ECNFs without electrical stimulation also showed a 2.4-fold higher than that of TCP controls. Similarly, upregulated expression of late stage neuronal differentiation marker MAP2 was observed on ECNF scaffolds with and without electrical stimulation relative to cells on TCPs, demonstrating 2.2-fold and 1.6-fold upregulation, respectively. In contrast, the astrocyte marker GFAP expression was downregulated on both groups of ECNF scaffolds with and without electrical stimulation. However, the nestin expression was just downregulated on non-electrical stimulated cells on ECNFs. These results demonstrate that the ECNFs have inherent neuronal-inducing capabilities.

The phenotype of NSCs under different conditions was assessed by staining MAP2 (a mature neuron maker). Figure 8 shows the immunofluorescence results of MAP2 for the electrical stimulated and unstimulated cells after 7 days in culture. MAP2 was significantly more expressed and displayed a greater intensity when cells underwent electrical stimulation. Additionally, neurite extension and elongation were more distinguished in the electrically stimulated group (Figure 8, *B* and *C*).

Discussion

In this report, we fabricated a highly conductive ECNF scaffold for guiding NSC functions and regenerative medicine application. The controllable process of synthesizing ECNFs offers many advantages, such as the generation of nano-features of scaffolds. Nanoscale conductive materials more closely resemble the features of life building blocks, such as proteins, nucleic acids, lipids, and carbohydrates.²⁸ Thus, we postulated that nano-features of our ECNF scaffolds can directly regulate NSC growth and differentiation. Different from most of current developed carbon based nanoscale scaffolds which usually are fabricated by doping or depositing fragmentary conductive CNFs, CNTs, or graphene into bulk materials, our ECNF scaffold was generated with integrated network structure (Figure 2, B). Through an annealing process, the structures in original polymer which might impair cell growth were removed and the scaffold was fully carbonized endowing excellent electrical conductivity (Figure 3). More importantly, our ECNF scaffold presents excellent flexibility (supporting movie 1), making it an excellent substrate for neural tissue engineering.

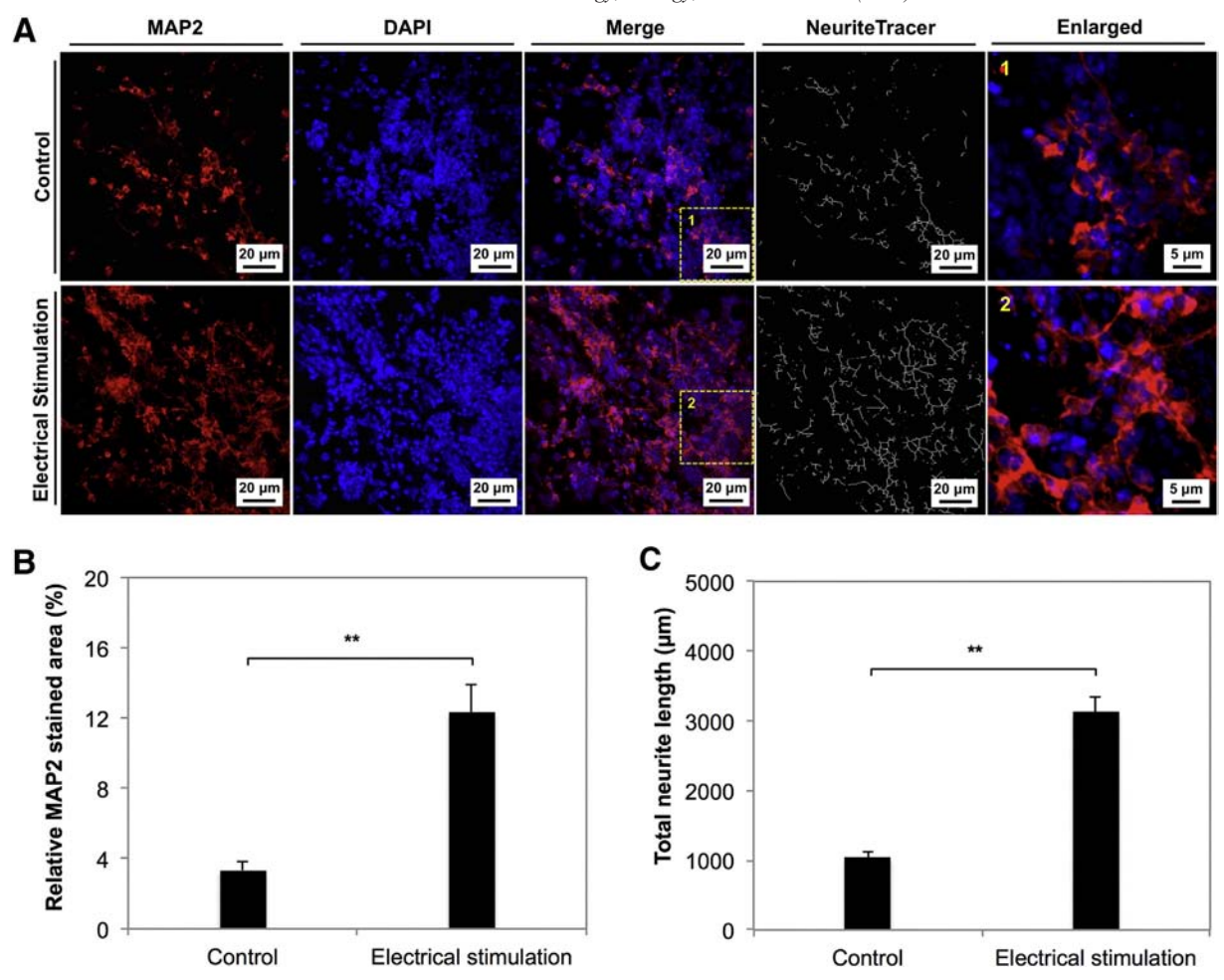


Figure 8. (A) Immunofluorescence micrographs of differentiated NSCs stained for the nuclei (blue) and neuronal marker MAP2 (red) in the presence and absence of electrical stimulation, and neurite outgrowth was traced by Neurite Tracer (ImageJ). Quantification of (B) relative MPA2 expression area and (C) total neurite length of NSCs with and without electrical stimulation. Data are reported as mean \pm standard deviation, n = 3, **P < 0.01.

When compared to cells on PAN scaffolds presenting relatively round morphology, the carbonized ECNF scaffolds supported robust cell spreading and well organized cytoskeletal fibers. This improvement might partially contribute to the graphitic structure of ECNFs formed by a carbonization treatment. After annealing, PAN yielded a graphitic structure similar to CNTs. ²⁹ The π -electron clouds in this structure have been reported to facilitate the ECM protein adsorption and result in minimal conformational change, which improved the cell adhesion to the surface of scaffolds. Importantly, the carbonized ECNF scaffolds process excellent conductive properties, allowing introducing external electrical stimulation to interact with the cells on them. Both *in vitro* and *in vivo* results revealed the effectiveness of direct electrical stimulation as a relatively simple, flexible strategy on improving cell or tissue functions. ^{31,32}

A biphasic current pulse has employed in several neural stimulation applications to stimulate the neural tissues for various diseases and injuries. ^{33–38} Particularly in our study, a magnitude of 100 uA biphasic current with 100 usec pulsed at 100 Hz exerted a significantly high cell proliferation on our electroactive ECNF scaffolds compared to that of PAN scaffolds. The biphasic current

used in our study holds several advantages when compared with direct current, capacitive coupling and inductive coupling which are popularly used in tissue engineering for electrical stimulation. Such electrical stimulation waveforms and patterns are able to lower the risk of faradic by-products generation including hydrogen peroxide, free radicals, hydroxyl, etc., reduce the charged protein accumulation (which impedes current flow) around electrode surfaces, as well as avoid the increase of pH value when exerting stimulation.³⁹ The effect of electrical stimulation on cell proliferation has been reported when it was applied on adipose-derived stem cells (ADSC). 40 It was found that the electrical stimulation can upregulate the proliferating cell nuclear antigen (a DNA polymerase-associated protein) and extracellular signal-regulated kinases 1 and 2 (molecules typically involved in transduction of proliferative signals) pathways as well as enhance cell proliferation rate. 40 Meanwhile, the multi-potentiality of stem cells was not compromised by the promoted proliferation.

In addition to the proliferative effect, electrical stimulation is also able to modulate stem cell differentiation fate and neurite outgrowth. In use of NSCs for neural regeneration, it is preferable to direct cell differentiation more toward neurons than glial cells. 4,43 By applying electrical stimulation to annealed

ECNF scaffold, we discovered the enhanced neuronal differentiation of NSCs when compared to that of electrical stimulation absence and cells on TCPs as illustrated by the gene expression analyses (Figure 7). The immunofluorescence results also suggest that the electrically stimulated NSCs on ECNF scaffold have programmed their differentiation toward neuronal lineage (Figure 8). It has been demonstrated that the electrical stimulation can change the local electrical field of ECM molecules, resulting in increased fibronectin adsorption to electrically conducting scaffolds. 44 Fibronectin is a glycoprotein that plays crucial roles in cell attachment and neurite outgrowth. The electrical conducting properties of ECNFs can guarantee that electrical stimulation through this conductive scaffold would be predominantly concentrate on the area around the scaffold, permitting spatial control of stimulation. Another mechanism in the literature suggested that the depolarization caused by electrical stimulation influences neural cell differentiation. In neural stem cells, the intracellular fluid has different potential with extracellular fluid, and neurite outgrowth is induced by depolarization. ^{27,45} When external electrical stimulation exceeds a threshold, an extra depolarization that resulted from action potential will generate and lead to improved neurite extension. These alterations might contribute to the enhanced neuronal differentiation of NSCs grown on our ECNF scaffold and stimulated by an electrical current.

In conclusion, we fabricated a novel ECNF scaffold by annealing electrospun polymer fibers. The ECNFs exhibit high flexibility and excellent electrical conductivity. It was demonstrated the proliferation of NSCs was promoted on the ECNF scaffold with electrical stimulation. The ECNFs affect the NSCs' fate during differentiation, illustrating the upregulated neuronal differentiation. More mature neurons were also observed in the electrically stimulated group. The findings showed great promise in use of combining ECNFs as conducting microenvironments and electrical stimulation for neural tissue engineering.

Appendix A. Supplementary data

Supplementary data to this article can be found online at http://dx.doi.org/10.1016/j.nano.2017.03.018.

References

- Pluchino S, Martino G. The therapeutic potential of neural stem cells. Nat Rev Neurosci 2006;7:395-406.
- Lindvall O, Kokaia Z, Martinez-Serrano A. Stem cell therapy for human neurodegenerative disorders - how to make it work. Nat Med 2004;10:S42-50.
- Yang N, Wernig M. Harnessing the stem cell potential: a case for neural stem cell therapy. Nat Med 2013;19:1580-1.
- Yang K, Lee JS, Kim J, Lee YB, Shin H, Um SH, et al. Polydopaminemediated surface modification of scaffold materials for human neural stem cell engineering. *Biomaterials* 2012;33:6952-64.
- Lee SJ, Zhu W, Heyburn L, Nowicki M, Harris B, Zhang L. Development of novel 3D printed scaffolds with core-shell nanoparticles for nerve regeneration. *IEEE Trans Biomed Eng* 2016 [PP:1-].
- Zhu W, Masood F, O'Brien J, Zhang LG. Highly aligned nanocomposite scaffolds by electrospinning and electrospraying for neural tissue regeneration. *Nanomedicine* 2015;11:693-704.

- Zhu W, O'Brien C, O'Brien JR, Zhang LG. 3D nano/microfabrication techniques and nanobiomaterials for neural tissue regeneration. *Nanomedicine* (Lond) 2014;9:859.
- Aldinucci A, Turco A, Biagioli T, Toma FM, Bani D, Guasti D, et al. Carbon nanotube scaffolds instruct human dendritic cells: modulating immune responses by contacts at the nanoscale. *Nano Lett* 2013;13:6098-105.
- Zhang L, Webster TJ. Nanotechnology and nanomaterials: promises for improved tissue regeneration. Nano Today 2009;4:66-80.
- Lovat V, Pantarotto D, Lagostena L, Cacciari B, Grandolfo M, Righi M, et al. Carbon nanotube substrates boost neuronal electrical signaling. *Nano Lett* 2005;5:1107-10.
- Matsumoto K, Shimizu N. Activation of the phospholipase C signaling pathway in nerve growth factor-treated neurons by carbon nanotubes. *Biomaterials* 2013;34:5988-94.
- 12. Fattahi P, Yang G, Kim G, Abidian MR. A review of organic and inorganic biomaterials for neural Interfaces. *Adv Mater* 2014;26:1846-85.
- Usmani S, Aurand ER, Medelin M, Fabbro A, Scaini D, Laishram J, et al.
 meshes of carbon nanotubes guide functional reconnection of segregated spinal explants. Sci Adv 2016;2 [e1600087-e].
- Park SY, Park J, Sim SH, Sung MG, Kim KS, Hong BH, et al. Enhanced differentiation of human neural stem cells into neurons on graphene. Adv Mater 2011;23:H263-7.
- Solanki A, Chueng STD, Yin PT, Kappera R, Chhowalla M, Lee KB. Axonal alignment and enhanced neuronal differentiation of neural stem cells on graphene-nanoparticle hybrid structures. *Adv Mater* 2013:25:5477-82.
- Tang M, Song Q, Li N, Jiang Z, Huang R, Cheng G. Enhancement of electrical signaling in neural networks on graphene films. *Biomaterials* 2013;34:6402-11.
- Fabbro A, Scaini D, León V, Vázquez E, Cellot G, Privitera G, et al. Graphene-based Interfaces do not alter target nerve cells. ACS Nano 2016;10:615.
- Rauti R, Lozano N, León V, Scaini D, Musto M, Rago I, et al. Graphene oxide nanosheets reshape synaptic function in cultured brain networks. ACS Nano 2016;10:4459-71.
- Quigley AF, Razal JM, Thompson BC, Moulton SE, Kita M, Kennedy EL, et al. A conducting-polymer platform with biodegradable fibers for stimulation and guidance of axonal growth. Adv Mater 2009;21:4393-7.
- Das S, Sharma M, Saharia D, Sarma KK, Sarma MG, Borthakur BB, et al. In vivo studies of silk based gold nano-composite conduits for functional peripheral nerve regeneration. *Biomaterials* 2015;62:66-75.
- Mazzatenta A, Giugliano M, Campidelli S, Gambazzi L, Businaro L, Markram H, et al. Interfacing neurons with carbon nanotubes: electrical signal transfer and synaptic stimulation in cultured brain circuits. J Neurosci 2007;27:6931-6.
- Mirzaei E, Ai J, Ebrahimi-Barough S, Verdi J, Ghanbari H, Faridi-Majidi R. The differentiation of human endometrial stem cells into neuron-like cells on electrospun PAN-derived carbon nanofibers with random and aligned topographies. *Mol Neurobiol* 2016;53:4798-808.
- Ye T, Durkin DP, Hu M, Wang X, Banek NA, Wagner MJ, et al. Enhancement of nitrite reduction kinetics on electrospun Pd-carbon nanomaterial catalysts for water purification. ACS Appl Mater Interfaces 2016;8:17739-44.
- Zhang L, Aboagye A, Kelkar A, Lai C, Fong H. A review: carbon nanofibers from electrospun polyacrylonitrile and their applications. J Mater Sci 2014;49:463-80.
- Inagaki M, Yang Y, Kang F. Carbon nanofibers prepared via electrospinning. Adv Mater 2012;24:2547-66.
- Liu H, Cao C-Y, Wei F-F, Huang P-P, Sun Y-B, Jiang L, et al. Flexible macroporous carbon nanofiber film with high oil adsorption capacity. J Mater Chem A 2014;2:3557-62.
- Ghasemi-Mobarakeh L, Prabhakaran MP, Morshed M, Nasr-Esfahani MH, Ramakrishna S. Electrical stimulation of nerve cells using conductive nanofibrous scaffolds for nerve tissue engineering. *Tissue* Eng Part A 2009;15:3605-19.

- Webster TJ, Waid MC, McKenzie JL, Price RL, Ejiofor JU. Nanobiotechnology: carbon nanofibres as improved neural and orthopaedic implants. *Nanotechnology* 2004;15:48-54.
- Ryu S, Lee C, Park J, Lee JS, Kang S, Seo YD, et al. Three-dimensional scaffolds of carbonized polyacrylonitrile for bone tissue regeneration. *Angew Chem* 2014;126:9367.
- Namgung S, Kim T, Baik KY, Lee M, Nam J-M, Hong S. Fibronectincarbon-nanotube hybrid nanostructures for controlled cell growth. *Small* 2011;7:56-61.
- Anderson M, Shelke NB, Manoukian OS, Yu X, McCullough LD, Kumbar SG. Peripheral nerve regeneration strategies: electrically stimulating polymer based nerve growth conduits. Crit Rev Biomed Eng 2015;43:131.
- Leppik LP, Froemel D, Slavici A, Ovadia ZN, Hudak L, Henrich D, et al. Effects of electrical stimulation on rat limb regeneration, a new look at an old model. Sci Rep 2015;5:18353.
- McCaig CD, Rajnicek AM, Song B, Zhao M. Controlling cell behavior electrically: current views and future potential. *Physiol Rev* 2005;85:943-78.
- Merrill DR, Bikson M, Jefferys JG. Electrical stimulation of excitable tissue: design of efficacious and safe protocols. J Neurosci Methods 2005;141:171-98.
- 35. Jensen RJ, Rizzo III JF. Responses of ganglion cells to repetitive electrical stimulation of the retina. *J Neural Eng* 2007;4:S1-6.
- Lim JH, McCullen SD, Piedrahita JA, Loboa EG, Olby NJ. Alternating current electric fields of varying frequencies: effects on proliferation and differentiation of porcine neural progenitor cells. *Cell Reprogram* 2013;15:405-12.

- Chang KA, Kim JW, Kim JA, Lee SE, Kim S, Suh WH, et al. Biphasic electrical currents stimulation promotes both proliferation and differentiation of fetal neural stem cells. *PLoS One* 2011;6:e18738.
- 38. Luo X, Weaver CL, Zhou DD, Greenberg R, Cui XT. Highly stable carbon nanotube doped poly(3, 4-ethylenedioxythiophene) for chronic neural stimulation. *Biomaterials* 2011;32:5551-7.
- 39. Ercan B, Webster TJ. The effect of biphasic electrical stimulation on osteoblast function at anodized nanotubular titanium surfaces. *Biomaterials* 2010;**31**:3684-93.
- Hernández-Bule ML, Paíno CL, Trillo MÁ, Úbeda A. Electric stimulation at 448 kHz promotes proliferation of human mesenchymal stem cells. *Cell Physiol Biochem* 2014;34:1741-55.
- Kobelt LJ, Wilkinson AE, McCormick AM, Willits RK, Leipzig ND. Short duration electrical stimulation to enhance neurite outgrowth and maturation of adult neural stem progenitor cells. *Ann Biomed Eng* 2014;42:2164-76.
- Yamada M, Tanemura K, Okada S, Iwanami A, Nakamura M, Mizuno H, et al. Electrical stimulation modulates fate determination of differentiating embryonic stem cells. Stem Cells 2007;25:562-70.
- 43. Gage FH. Mammalian neural stem cells. Science 2000;287:1433-8.
- Kotwal A, Schmidt CE. Electrical stimulation alters protein adsorption and nerve cell interactions with electrically conducting biomaterials. *Biomaterials* 2001;22:1055-64.
- Howe CL. Depolarization of PC12 cells induces neurite outgrowth and enhances nerve growth factor-induced neurite outgrowth in rats. *Neurosci Lett* 2003;351:41-5.